ELSEVIER

Nuclear Instruments and Methods in Physics Research A 457 (2001) 212–219

NUCLEAR INSTRUMENTS & METHODS IN PHYSICS RESEARCH Section A

www.elsevier.nl/locate/nima

Response function of a germanium detector to photon energies between 6 and 120 keV

J.Y. Zevallos-Chávez[a], M.T.F. da Cruz[a], M.N. Martins[a,*], V.P. Likhachev[a], C.B. Zamboni[b], S.P. Camargo[b], F.A. Genezini[b], J.A.G. Medeiros[b], M.M. Hindi[c]

[a]*Instituto de Física da Universidade de São Paulo, Rua do Matão, Travessa R 187 05508–900 São Paulo, SP, Brazil*
[b]*Instituto de Pesquisas Energéticas e Nucleares, IPEN/CNEN-SP, Brazil*
[c]*Tennessee Technological University, Cookeville, TN 38505, USA*

Received 18 August 1999; received in revised form 14 December 1999; accepted 11 May 2000

Abstract

We have developed a function to describe the response of an 8-cm^3 germanium detector to photon energies as low as 6 keV, going up to 120 keV. Detection effects like the Ge X-ray escape and Compton scattered photons in the neighborhood of the detector were treated. This study was based on the fit of analytic functions to the features of the experimental spectra, thus revealing the parameters and their dependence on the photon energy. Our response function has 13 parameters and its validity is shown by the reproduction of the parameter-generating spectra and through the independent fit of an ^{152}Eu spectrum.

1. Introduction

Knowledge of the response function of a gamma-ray spectrometer is important to make accurate assumptions about the actual distribution of intensities, as in the analysis of continuous spectra. An example is the study of the inner bremsstrahlung accompanying electron-capture decay.

The main motivation for this work was the lack of a treatment of the low photon energy region (from a few keV up to about 100 keV). There are various approaches for designing response functions (Monte Carlo calculations, analytic expressions, transformations together with linear combinations of previously stored experimental spectra, etc.) and we have chosen that of taking relatively simple experimental spectra, fitting their relevant features with the help of suitable analytic functions, and studying the dependence of the parameters of the fit with the photon energy. Another criterion adopted was that of replacing any mathematical folding required by the physical process by an empirical analytic form (e.g. this is the case with the multiple-Compton scattering and the incomplete charge collection effects [1,2]).

At such low photon energies it is advisable to use sources to produce the response function with similar mounting to that of the sources that will be studied. In this work we have used a 32-mm-diameter and 10-mm-thick planar Ge crystal, with a 0.3-μm-thick frontal dead layer.

* Corresponding author. Fax: 55-11-81-86832.
E-mail address: martins@if.usp.br (M.N. Martins).

0168-9002/01/$ - see front matter
PII: S0168-9002(00)00702-6

2. The response function

Detection effects at low photon energies, such as the Ge X-ray escape peaks and photons Compton-scattered in the neighborhood of the detector, especially at the detector crystal holder, deserved a careful treatment. Some of the functions shown here have already been used before [1,2] and work well, although a certain tuning is needed, depending on the photon energy, as will be discussed.

The response function describing the interactions of a photon of energy E_γ will be written as

$$R(E,E_\gamma)=\sum_{i=1}^{7} f_i(E,E_\gamma) \tag{1}$$

where E is the energy argument of R. The seven pieces, f_i, of the response function and their parameters, which depend on the photon energy, are described below. We also briefly discuss their characteristics, comparing in some cases to what was done in previous works [1–3]. Finally, the response function for this type of detector is written.

2.1. Photopeak

The full absorption of a photon will be represented by a Gaussian distribution with amplitude p_1, centroid at E_γ (fixed) and full-width at half-maximum (FWHM) p_2:

$$f_1(E,E_\gamma)=p_1\times\exp\left[-\left(\frac{E-E_\gamma}{0.6005\times p_2}\right)^2\right] \tag{2}$$

where p_2 depends on the photon energy. All other features of the spectrum will have amplitudes (or intensities) fitted relative to the photopeak amplitude, p_1.

2.2. Incomplete charge collection

The effect of incomplete charge collection shows up a tailing on the low-energy side of the photopeak. There are two components for this:

(1) The first one comes from charge carrier trapping [1,2] in crystal defects with their delayed release. This is expressed here as

$$f_2(E,E_\gamma)=p_1\times p_3\times\exp\left(\frac{E-E_\gamma}{\pi\times 0.6005\times p_2\times p_4}\right)\times\operatorname{erfc}\left(\frac{E-E_\gamma}{0.6005\times p_2}+\frac{1}{2\times p_4}\right) \tag{3}$$

where p_3 is the relative amplitude of this effect. The exponential term generates the exponential low-energy tail and the complementary error function (erfc) kills f_2 under the photopeak, at a certain distance of its centroid, E_γ. The parameter p_4 is related to the slope and centroid of f_2 under the photopeak [2].

(2) The second component is mainly related to the escape of photoelectrons [4] and bremsstrahlung from the active volume of the detector, and is described as a constant plateau or step down to low energies, smoothly decreasing to zero under the photopeak. This is achieved by convoluting a constant function with a Gaussian, resulting [1] in

$$f_3(E,E_\gamma)=p_1\times p_5\times\tfrac{1}{2}\times\operatorname{erfc}\left(\frac{E-E_\gamma}{0.6005\times p_2}\right) \tag{4}$$

where p_5 is the relative amplitude of this effect and the factor $\frac{1}{2}$ corrects for the limit of the complementary error function far from its decaying region (which is 2).

2.3. Compton scattering in the detector

Compton scattering of photons is usually described by the Klein–Nishina cross section [5]. As can be seen from the experimental data (see Fig. 1), one must take into account the momentum distribution of the bound electron, responsible for the rounding, or smoothing, of the Compton edge and the introduction of some slope in its abrupt drop [6]. This effect is enhanced towards low photon energies.

The Compton structure was then described by the Klein–Nishina expression multiplied by a complementary error function that dies close to the Compton edge energy, E_c. The form below proved to be suitable and presents two differences to the expression of Myung et al. [1]: (1) we have the half-value decrease of the complementary error function occurring exactly at the Compton edge,

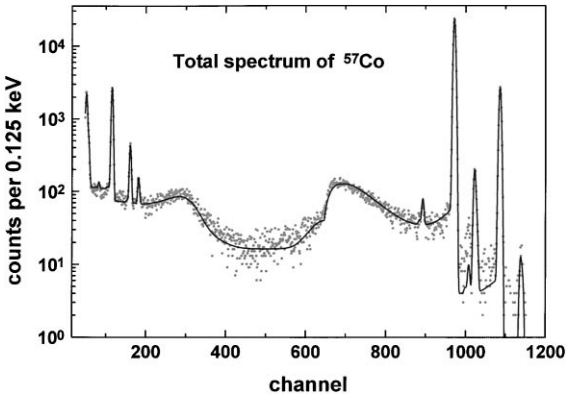

Fig. 1. ^{57}Co spectrum, measured (data points) and fitted (solid line). The χ^2_v value for this fit was 1.4.

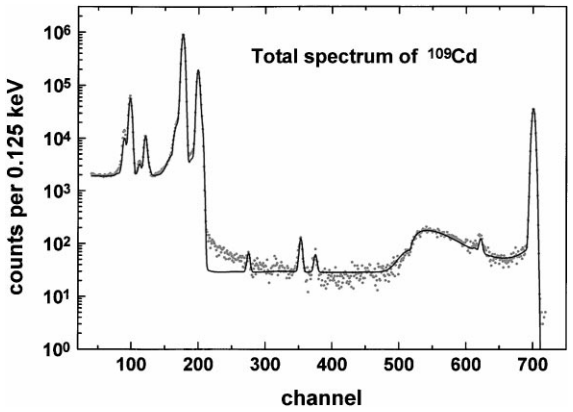

Fig. 2. ^{109}Cd spectrum, measured (data points) and fitted (solid line). The χ^2_v value for this fit was 49. Some sum peaks were included.

E_c, which is fixed, instead of attributing an extra parameter for that purpose, and (2) the Compton structure is not restricted to go to zero for energies above E_c, but is let to fade smoothly, as an approximation to the contribution of multiple Compton scattering,

$$f_4(E,E_\gamma) = p_1 \times p_6 \times \left(\frac{E_\gamma}{E-E_\gamma} + \frac{E-E_\gamma}{E_\gamma} - 1 + \cos^2\theta\right) \times \operatorname{erfc}\left(\frac{E-E_c}{\sqrt{2}\times p_7}\right) \quad (5)$$

where

$$\cos\theta = \frac{m_e c^2}{E-E_\gamma} + 1 + \frac{m_e c^2}{E} \quad (6)$$

and

$$E_c = \frac{E_\gamma}{1 + m_e c^2/2E_\gamma} \quad (7)$$

is the Compton edge energy and $m_e c^2$ is the rest energy of the electron. In Eq. (5), p_6 is the relative amplitude and p_7 is related to the width of the rounding effect.

2.4. Compton scattering in the neighborhood

As the photon energy goes below $m_e c^2/2 \approx$ 250 keV, the Compton continuum and the back-

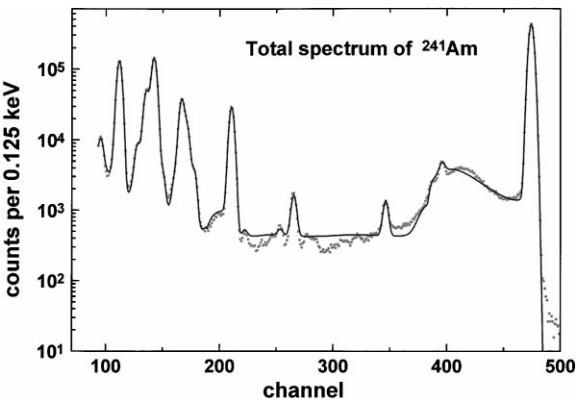

Fig. 3. ^{241}Am spectrum, measured (data points) and fitted (solid line). The χ^2_v value for this fit was 30. Some sum peaks were included.

scattering structure exchange their positions, the latter appearing at a higher energy. When measuring photons with a solid-state X-ray detector, like a Ge or Si(Li), the experimental spectrum usually shows a hump to the left of the photopeak, identified as the Compton scattering of photons in the vicinity of the detector crystal (backscattering) with their subsequent detection. This structure can be seen in Figs. 1–4, taken with different calibration sources. Since this structure extends from a minimum energy up to the photopeak itself, small-angle scattering is also present, and could take

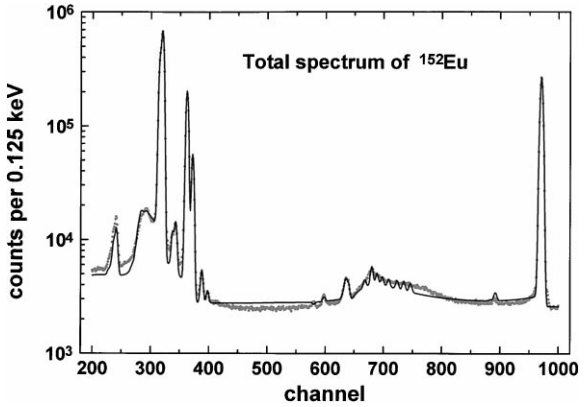

Fig. 4. ^{152}Eu spectrum, measured (data points) and fitted (solid line). The χ^2_ν value for this fit was 82. This fit shows the validity of the proposed response function. Some sum peaks were included.

place in the source, for instance. The low-energy end of the hump corresponds to photons of energy $E_\gamma - E_c$, produced by those of initial energy E_γ, Compton scattered at 180°. Calculations and simulations with the EGS4 code [7], have shown that the main contribution to this effect comes from the detector holder, inside the end cup, like the copper cold finger, etc. We have used a cylindrical graded shield (25 cm long and about 12 cm internal diameter, with a 2-cm-thick Pb outer layer and a 5-mm-thick Cu inner one) and the contribution of photons reaching the detector after being scattered in the shield was negligible. We have chosen to simulate its shape as a Dawson integral [8, Fig. 7.2, on p. 297], but modified as

$$f_5(E,E_\gamma)=\begin{cases} p_1\times p_8\times\exp(-y)\times\operatorname{erf}(y) & \\ \times\frac{1}{2}\times\operatorname{erfc}\left(\dfrac{E-E_\gamma}{0.6005\times p_2}\right), & y>0 \\ 0, & y\le 0 \end{cases} \quad (8)$$

where y comes from the linear transformation

$$y=p_9\times\left(\frac{E-E_{\min}}{E_\gamma-E_{\min}}\right) \quad (9)$$

with

$$E_{\min}=E_\gamma-E_c-p_{10}. \quad (10)$$

p_8 is the relative amplitude and y is the proper coordinate of the modified Dawson function, given by the product $\exp(-y)\times\operatorname{erf}(y)$. The parameter y also controls the shape of the structure through the scaling factor p_9, and the complementary error function in Eq. (8) is there to assure that the structure vanishes under the photopeak. Finally, p_{10} represents a small amount of freedom given to the low-energy end of the structure, that should be the energy of the 180° Compton-scattered photons, represented by $E_{\min}$.

We have added a Gaussian function to the low-energy end of the hump, given by

$$f_6(E,E_\gamma)=p_1\times p_{11}\times\exp\left[-\frac{1}{2}\left(\frac{E-E_{\min}}{p_{12}}\right)^2\right]\times\frac{1}{2}\times\operatorname{erfc}\left(\frac{E-E_\gamma}{0.6005\times p_2}\right) \quad (11)$$

where p_{11} is the relative amplitude, p_{12} is the width parameter of the Gaussian with centroid at $E_{\min}$ and the complementary error function has the same role as in Eq. (9). The role of this Gaussian is to produce a tail on the hump. Such a tail is not necessary for very low photon energies, $E_\gamma < 40$ keV, because the hump itself grows thinner (but still with observable amplitude), with its low-energy side closing up to the photopeak as the photon energy decreases.

2.5. Ge X-ray escape peaks

The characteristic X-rays of the detector material are generated during the photon interactions inside the active volume and may escape this volume, especially if they are generated close to the surface. When this happens, less energy is collected by the detector. It is, in general, observed at low photon energies ($\lesssim$200 keV), as a pair of small peaks to the low-energy side of the photopeak, at the energies $E_\gamma - E_{K\alpha}$ and $E_\gamma - E_{K\beta}$. In the case of germanium detectors these energies are $E_{K\alpha} = 9.87$ keV and $E_{K\beta} = 10.98$ keV with a relative fluorescence yield of $Y_{K\beta}/Y_{K\alpha} = 0.129$ [9]. We describe these peaks as two Gaussians with centroids at $E_\gamma - E_{K\alpha}$ and $E_\gamma - E_{K\beta}$, with an amplitude ratio given by

$Y_{K\beta}/Y_{K\alpha}$. This term is written

$$f_7(E,E_\gamma)=p_1\times p_{13}\times\left\{\exp\left[-\left(\frac{E-(E_\gamma-E_{K\alpha})}{0.6005\times p_2}\right)^2\right]+0.129\times\exp\left[-\left(\frac{E-(E_\gamma-E_{K\beta})}{0.6005\times p_2}\right)^2\right]\right\}, \quad (12)$$

where p_{13} is their relative amplitude.

3. Experiment

Since the energy range of interest is quite low, the spectra might display features due to some characteristics of the sources, like self-absorption, absorption in the source protective window, photon scattering on the aluminum ring holder, etc. For this reason we describe the radioactive sources used in this work and the experimental setup as well.

3.1. Source preparation

The radioactive sources used in the parameter mapping and also for the final check were prepared at the Laboratório de Metrologia of the IPEN/CNEN-SP. The isotopes used were ^{57}Co, ^{109}Cd, ^{241}Am and ^{152}Eu. Their sources had activities ranging from 0.1 to 0.5 μCi, except for the ^{57}Co source, whose activity was about 0.02 μCi. The sources were prepared by the droplet technique: a few drops of the radioactive source were deposited on the center of a circular polyethylene foil 0.4-mm-thick, dried with the help of a gentle nitrogen gas blow. Once dried, they were covered with another polyethylene foil. For some sources this cover was 0.4-mm-thick and for others only 0.1-mm-thick, resulting in a front window absorption of only about 4–5% at 8 keV photon energy. Each source was held with the help of a pair of aluminum rings clipping the edges of the polyethylene sheets, then sealing the radioactive materials. The mounting diameter was 30 mm and the source diameter (i.e. the diameter of the deposit) was about 10 mm.

3.2. Experimental setup

The Ge X-ray detector, made by EG&G ORTEC, was composed by a 32-mm-diameter and 10-mm-thick planar Ge crystal, with a 0.3-μm-thick frontal dead layer. The crystal is enclosed in a horizontal-type cryostat, with an aluminum end-cup and a 0.25-mm-thick Be window and operates at −1000 V bias. This detector was put inside an iron shield shaped as a hollow cylinder, 43-cm-long and with 10.3 cm internal diameter. The iron thickness was 10.1 cm. The sources were held by a plastic holder, and the source to detector distance could be chosen between 2 and 6 cm.

The setup used standard nuclear spectroscopy electronics, composed by an Ortec 572 amplifier, where the unipolar and pile-up rejection (PUR) outputs were used respectively as the linear (for pulse-height analysis, PHA) and gate inputs to a PC-based Ortec ADCAM®, AD811. The last signal was used to perform an anti-coincidence, thus removing the tail piled-up events. The unrejected pile-up rates, mainly among characteristic X-rays of the sources, were $5\times10^{-2}\,s^{-1}$ for ^{241}Am and ^{152}Eu, $10^{-3}\,s^{-1}$ for ^{109}Cd, and negligible for ^{57}Co. The 4096-channel PHA spectra presented a typical energy gain of about one-eighth of keV per channel.

3.3. Spectrum analysis

A set of background-subtracted spectra was prepared, keeping track of the error propagation. The analyses of these spectra were performed within the framework of MATLAB®, where a complete set of routines was written to perform a least-squares fit of the response function, based on the Gauss–Marquardt algorithm [10, See routine CURFIT]. Due to particularities of the data, like the presence of characteristic X-rays, the fits were not done seeking for new or better photon energy values. We did a simultaneous fit of a linear energy calibration to the spectra, keeping the energies of the known photopeaks fixed at the values quoted in the literature [9].

The fitting procedure was a two-step process: (1) the parameters present in the response function were determined for several photon energies by

fitting the experimental spectra of various sources; (2) the dependence of those parameters with the photon energy was also fit, using either physically reasonable or empirical functions. In the first stage the response function contained 13 energy-dependent parameters, p_j. After the second step, these became 13 functions, the response function depending only on the incident photon energy. In other words, once the photon energy is known, the detector response is completely determined by the photopeak energy and scaled by the photopeak area.

Finally, in order to test our response function model, we have refitted the spectrum of each source, obtaining a good agreement. In Figs. 1–3 we show the total spectra for ^{57}Co, ^{109}Cd and ^{241}Am, respectively. Some of the peaks appearing in intermediary regions were not modelled, i.e., were not introduced in the calculations for they are peak pile-up effects. Furthermore, we have obtained good agreement between the model response function and the data when fitting an ^{152}Eu spectrum, which did not participate in the parameter-mapping procedure. Fig. 4 shows the results.

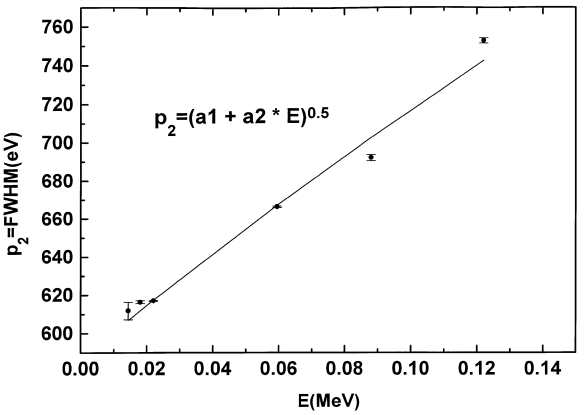

Fig. 5. Fit of p_2, the full width at half maximum.

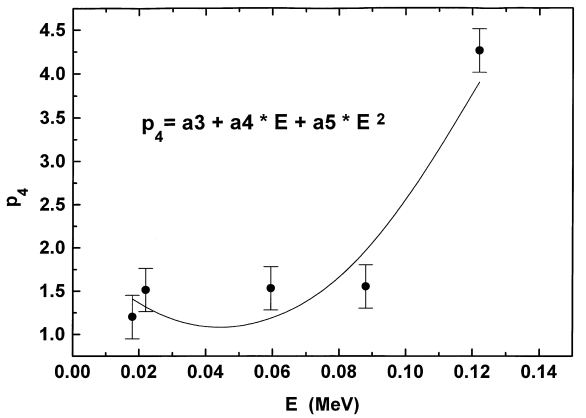

Fig. 6. Fit of p_4, related to f_2, one of the incomplete charge collection terms.

4. Conclusions

We have performed a semi-empirical calculation of the response of an 8 cm^3 hiper-pure germanium X-ray detector in the energy range 6–120 keV.

The values of the 13 parameters obtained for the photons emitted by the calibration sources ^{57}Co, ^{109}Cd and ^{241}Am allowed the study of these values as functions of the photopeak energy, E_γ, as can be seen from Figs. 5–10.

This allowed us to choose simple functions of the photopeak energy, E_γ, like constant, straight line or parabola for most of the parameters. An exception was the Compton relative amplitude, p_6, which was hard to determine because this structure at low energies is usually buried under the characteristic X-rays, except for the ^{57}Co source, where a reliable value for p_6 was obtained. In this case, we have fitted the experimental values of the Compton scattering cross section for germanium, found in the literature, and normalized the fit at the energy of 122.061 keV of ^{57}Co, so that the value at that energy reproduces the value we want for p_6, and took the normalized fit as our p_6 dependence on the photon energy. The continuous lines shown in Figs. 5–10 are the fits done for some of the parameters, and Table 1 contains the functions used and the resulting values of their parameters.

Some of the parameters have shown little or no dependence with the photon energy, as can be seen from Table 1. In particular, p_{10} (the small walk of the low energy end of the backscattering hump) and

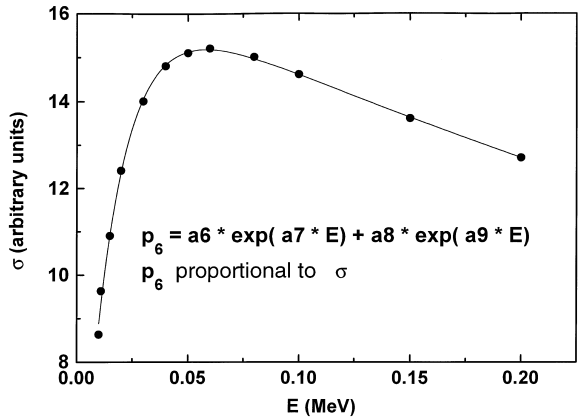

Fig. 7. Fit of p_6, the coefficient of the Compton scattering cross section. This fit was normalized at the 122.1-keV line in the ^{57}Co spectrum, to produce the appropriate amplitude.

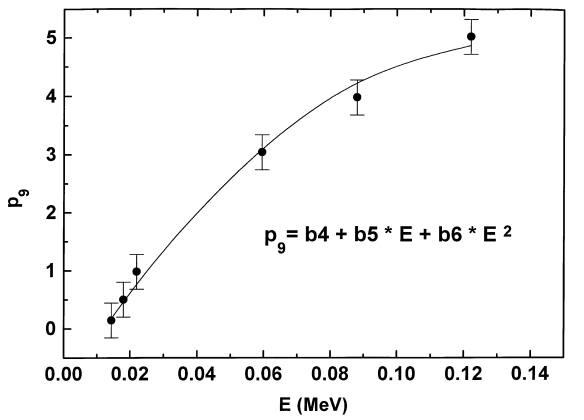

Fig. 9. Fit of p_9, coefficient of the linear transformation in the modified Dawson function, f_5.

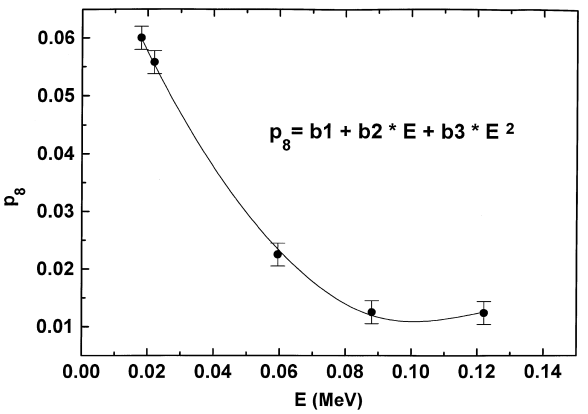

Fig. 8. Fit of p_8, the coefficient of the Compton scattering in the neighborhood of the detector.

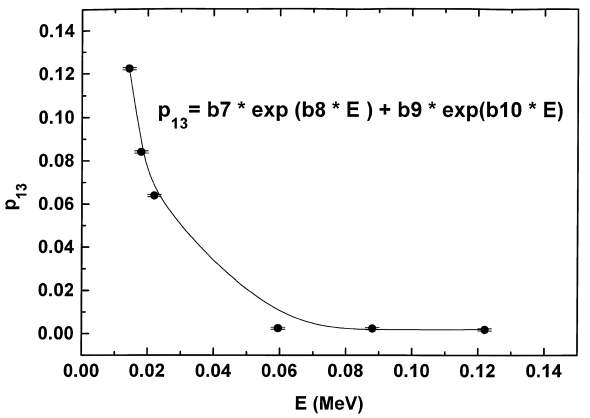

Fig. 10. Fit of p_{13}, the coefficient of the Ge X-ray escape peaks.

p_{12} (the width of the Gaussian placed at the low-energy end of the backscattering hump) show very little sensitivity to the photon energy at X-ray energies (i.e. $E_\gamma \lesssim 30$ keV) and this is explained by the abruptness of the corresponding structure at those low energies.

A look at the reduced chi-square values of the fits, χ^2_ν, presented in Figs. 1–5 reveals that some are somewhat poor, but one should bear in mind that the modelled response function does not contain exact formulations for multiple Compton scattering, for instance, and that the contributions coming from the higher-energy gamma rays were taken only approximately into account, via a constant or higher-order polynomial background when needed. That was the case for ^{152}Eu. Another issue is the presence of characteristic X-rays at the low-energy part of the range under study, making the analysis rather complex.

On balance, the description of the experimental spectra using our response function is faithful enough for our purposes, the study of low-energy inner bremsstrahlung data.

Table 1
Meaning and functional form of the parameters as functions of the photopeak energy, E_γ, in MeV

Parameter	Meaning	Functional form
p_1	Photopeak amplitude	Fit for each photopeak
p_2	Photopeak FWHM (MeV)	$\sqrt{3.44\times10^{-7}+1.70\times10^{-6}E_\gamma}9.27\times10^{-4}$
p_3	Incomplete collection coefficient	
p_4	Incomplete collection centroid/slope	$2.01-41.7E_\gamma+4.68\times10^{2}E_\gamma^2$
p_5	Plateau coefficient	$1.54\times10^{-3}\exp(-7.25E_\gamma)+6.04\exp(-4.59\times10^{2}E_\gamma)$
p_6	Compton coefficient	$1.11\times10^{-3}\exp(-1.40E_\gamma)-1.02\times10^{-3}\exp(-67.8E_\gamma)$
p_7	Compton edge rounding width	$4.60\times10^{-3}E_\gamma+1.86\times10^{-1}E_\gamma^2$
p_8	Backscattering coefficient	$8.28\times10^{-2}-1.40E_\gamma+6.75E_\gamma^2$
p_9	Backscattering scale factor	$-1.04+89.2E_\gamma-3.35\times10^{2}E_\gamma^2$
p_{10}	Backscattering start shift	$5.38\times10^{-4}-1.72\times10^{-2}E_\gamma+2.02\times10^{-1}E_\gamma^2$
p_{11}	Backscattering rounding coefficient	$2.92\times10^{-3}-2.43\times10^{-2}E_\gamma+6.70\times10^{-2}E_\gamma^2$
p_{12}	Backscattering rounding width	$1.55\times10^{-3}-4.38\times10^{-2}E_\gamma+5.35\times10^{-1}E_\gamma^2$
p_{13}	Ge X-ray escape peaks coefficient	$7.91\times10^{-4}\exp(7.35E_\gamma)+4.73\times10^{-1}\exp(-94.5E_\gamma)$

Acknowledgements

We acknowledge the support by Fundação de Amparo à Pesquisa do Estado de São Paulo, FAPESP, Conselho Nacional de Desenvolvimento Científico e Tecnológico, CNPq, and Co-ordenação de Aperfeiçoamento de Pessoal de Nível Superior, CAPES.

References

[1] C. Lee Myung, K. Verghese, R.P. Gardner, Nucl. Instr. and Meth. A 262 (1987) 430.
[2] R.P. Gardner, J.M. Doster, Nucl. Instr. and Meth. 198 (1982) 381.
[3] J.L. Campbell, H.H. Jorch, Nucl. Instr. and Meth. 159 (1979) 163.
[4] L.A. McNelles, J.L. Campbell, Nucl. Instr. and Meth. 127 (1975) 73.
[5] R.D. Evans, The Atomic Nucleus, McGraw-Hill, New York, 1955.
[6] J. Felsteiner, S. Kahane, B. Rosner, Nucl. Instr. and Meth. 118 (1974) 253.
[7] W.R. Nelson, H. Hirayama, D.W.O. Rogers, The EGS4 code system, SLAC Report 265, 1985.
[8] M. Abramowitz, I.A. Stegun, Handbook of Mathematical Functions, 9th Edition, Dover, New York, 1970.
[9] R.B. Firestone, E. Browne, Table of Radioactive Isotopes, Wiley, New York, 1986.
[10] P.R. Bevington, Data Reduction and Error Analysis for the Physical Sciences, McGraw-Hill, New York, 1969.